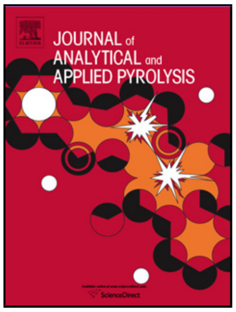

Title: Kinetics of the combustion of olive oil. A semi-global model

Author: Rafael Font María D. Rey María A. Garrido

PII: S0165-2370(14)00121-1
DOI: http://dx.doi.org/doi:10.1016/j.jaap.2014.05.015
Reference: JAAP 3207

To appear in: *J. Anal. Appl. Pyrolysis*

Received date: 17-12-2013
Revised date: 14-3-2014
Accepted date: 12-5-2014

Please cite this article as: R. Font, M.D. Rey, M.A. Garrido, Kinetics of the combustion of olive oil. A semi-global model, *Journal of Analytical and Applied Pyrolysis* (2014), http://dx.doi.org/10.1016/j.jaap.2014.05.015

Kinetics of the combustion of olive oil. A semi-global model

Rafael Font*, María D. Rey, María A. Garrido

Chemical Engineering Department, University of Alicante, P.O. Box 99, 03080
Alicante, Spain

1. INTRODUCTION

The increasing need of energy by segments of our society, the reduction of petroleum reserves and increased environmental concerns have caused biomass materials to gain much interest with respect to energy utilization. For example, waste vegetable oils can through thermal decomposition be used to directly obtain energy or fuels [1]. It is very important to perform thermal analysis of the oils to predict their behavior in real combustion systems. The combustion kinetics of these fuels gives relevant information on their thermal behavior and on the possible formation of a carbonaceous residue and its subsequent oxidation.

Jansson et al. [2] studied the pyrolysis of olive oils and other vegetable oils, and determined the evolved compounds on a Pyrolyzer/GC/MS. Gases such as propene and liquids such as oleic acid, docosene and octadecenal, with boiling points at around 360 ºC (633 K), were found. In a combustion process these compounds are oxidized, which changes the composition of the gas phase.

The subject of a previous paper was a study of the pyrolysis kinetics of olive and used olive oil [3]. The pyrolytic decomposition was analyzed taking into consideration the vaporization process involved, and the results were compared with a number of kinetic considerations discussed in other papers [4-6]. The proposed kinetic model considered two sequential processes: a first process, considering vaporization and decomposition, whose apparent activation energy and reaction order were 112 kJ/mol and 0.606, respectively, and a second process, whose apparent activation energy and reaction order were 194.6 kJ/mol and 2.274, respectively. The values obtained in both of these processes are acceptable; in the first process, the values are between those of the vaporization process and chemical decomposition, and in the second they were common values for decomposition processes.

Others have also studied the oxidative thermal decomposition in order to characterize vegetable oils [7,8]. Tran et al. [9] examined a number of mechanisms of the combustion of oxygenated compounds of biofuels.

Dweck and Sampaio [10] analyzed the thermal decomposition of commercial vegetable oils by TG/DTA and observed four decomposition steps. They proposed that the last one corresponds to the burnout of the residual carbonaceous material.

Concerning the global kinetics, Vecchio et al. [7] studied the oxidative thermal decomposition of single-varietal extra olive oil by TG/DSC, and observed a complex multistep decomposition. They attributed the first apparent peak to two different processes for the purpose of relating them to the chemical composition. From the first decomposition step they obtained apparent activation energies for the de-convoluted peaks ranging between 27 and 158 kJ/mol, and 31 and 278 kJ/mol for the first and second peaks, respectively. No other information concerning kinetic parameters was presented.

Gouveia de Souza et al. [11] elucidated the oxidation kinetics of sunflower oil by TG, by considering three decomposition steps in which the interaction of the oxidation reactions was important. The first step takes place between 503 and 653 K with reaction order around 1 and activation energy around 90-110 kJ/mol, in which the volatile compounds were removed by the vapor generated during heating. The second is between 653 and 753 K with reaction order around 2 and activation energy of 205-300 kJ/mol. The third step takes place between 753 and 823 K and the deduced reaction orders and apparent activation energies were around 2 and 300-400 kJ/mol, respectively.

Santos et al. [12] considered three decomposition steps in the oxidative decomposition of a number of edible oils, including olive oil. Similar kinetic parameters were obtained. In the first step, the apparent activation energy was between 78 and 106 kJ/mol and the reaction order was between 0.92 and 1.06. In the second step, the apparent activation energy was between 208 and 349 kJ/mol and the reaction order was between 1.86 and 2.11. In the last step, an activation energy between 274 and 370 kJ/mol and a reaction order between 1.87 and 2.13 were obtained. No values were reported for the mass fractions of the volatiles evolved in each step.

Zhengwen [13] recently studied the combustion of cooking oil tar on a TG apparatus. He observed four DTG peaks after the initial evaporation of the absorbed water, and made several plots for correlating the data which suggest a model of First Order Reaction and Three-dimensional Diffusion Separate-stage. However, values for the apparent activation energy were not reported.

Vecchio et al. [14] studied the decomposition of triglycerides contained in olive oil by TG. They observed the presence of four decomposition steps and determined the kinetic parameters of the first two decomposition steps.

More recently, Tomassetti et al. [15] analyzed the thermal decomposition of saturated mono-, di- and tri-glycerides. They also observed four decomposition steps and proposed the kinetic parameters for the two or three first steps.

The decomposition kinetics of complex materials (synthetic polymers, biomass, oils, etc.) is a subject that deals with the examination and analysis of kinetic parameters, with a view to clarifying their significance [16-18]. Thus, efforts to study the decompositions of substances such as vegetable oils can help to reduce the existing chaos in the field of reaction kinetics of complex materials.

In this paper, a kinetic model for the combustion of olive oil at air atmosphere and also in one that is oxygen-poor has been developed by simultaneous determination at each step of the kinetic parameters and the mass fraction of the volatiles. The experimental data are compared with those obtained by simulation using the deduced expressions. We also discuss the possibility of a carbonaceous residue formed during the thermal oxidation of the fuels in question, which has not been considered in previous papers. The kinetic study is analyzed by contrasting with the study on olive oil by Vecchio et al. [7], as well as other studies carried out on other vegetable oils. The kinetic model can be used to characterize certain decomposition steps of the edible oils and/or their corresponding wastes and to analyze the formation of a carbonaceous residue.   .

2. EXPERIMENTAL

2.1 Raw material

Pure olive oil, waste olive oil and waste mixed oil were selected as materials for studying the kinetics. This study employed the same pure olive oil as a previous pyrolysis kinetic study [3]. The waste olive oil was obtained after four/five frying processes, which corresponds to an average use of this oil, and was also the same waste olive oil employed in the previous pyrolysis kinetic study [3]. A waste mixed oil, consisting of a mixture of different used cooking oils, was also utilized to determine whether there are any great differences between the oils. An elemental analysis of the samples was carried out on a Perkin-Elmer 2400 to determine the mass fractions of carbon, hydrogen, nitrogen and sulphur; oxygen content was determined by a direct oxygen analysis carried out on a Flash-2000 Thermo Fisher Scientific; a LECO Instruments AC-350 calorimetric bomb was used to obtain the net calorific value. Table 1 shows the results of the elemental analysis and the net calorific values of the three samples tested. As observed, there are no big differences between the samples.

Table 1

2.2 Apparatus and experimental procedure

The combustion runs at air atmosphere were carried out on two different TG apparatus whereas in the N_2:O_2 = 9:1 runs only one of them was used:

1) A Mettler Toledo Thermobalance model TGA/SDTA851e/LF/1600. This instrument incorporates a horizontal furnace and a parallel-guided balance. In this way, positioning of the sample has no influence on the measurement, and flow gas perturbation and thermal buoyancy are minimized. The sample temperature was measured by a sensor directly attached to the sample holder. Two different atmospheres were used; N_2:O_2 = 4:1 and N_2:O_2 = 9:1. The crucibles employed in the runs were a nearly cylindrical aluminum crucible of 0.55 cm internal diameter and 0.41 cm height, which is slightly curved at the bottom of the cylinder, and a cylindrical alumina crucible of 0.47 cm internal diameter and 0.42 cm height.

2) A Perkin Elmer Thermobalance model TGA/SDTA-6000. This instrument incorporates a vertical furnace and a single beam vertical balance. As in the previous case, positioning of the sample has no influence on the measurement, and flow gas perturbation and thermal buoyancy are minimized. The SaTurnA sensor measures both

the sample and reference temperature directly for superb performance. The alumina crucible used in all runs was nearly cylindrical with 0.65 cm internal diameter and 0.42 cm height and was slightly curved at the bottom of the cylinder. Synthetic air was used as fluid, so these results can be compared with the results obtained at N_2:O_2 = 4:1 using the Mettler Toledo Thermobalance.

Dynamic experiments were carried out at heating rates between 5 and 20 K/min, from the initial room temperature up to 850 K, including thus the entire range of decomposition. Isothermal experiments started at a constant heating rate until the desired temperature was reached and then the final temperature was maintained constant. The experiment was considered to have finished when the weight loss rate was negligible (less than $1 \cdot 10^{-5}$ s^{-1}). Small size samples, between 1 and 10 mg, were used in the runs.

A pyrolysis run at a heating rate of 5 K/min using Avicel PH-105 microcrystalline cellulose was done on each apparatus. The kinetic parameter values obtained showed good agreement with the results reported by Grønli et al. [19] in their round-robin study of cellulose pyrolysis kinetics by thermogravimetry (at 5 K/min and 244 kJ/mol, the experimental and calculated data coincide, obtaining logarithmic values of the pre-exponential factors of around 18.8, a value within the accepted interval). These experiments were useful to check how well the two thermobalances performed.

The TG-MS runs were carried out on a Mettler Toledo model TG-ATD TGA/SDTA851e/LF/1600 coupled to a Thermostar GSD301T Pfeiffer Vacuum MS apparatus using He:O_2 = 4:1 as carrier gas. The operating conditions were: a mass sample of around 5 mg, a 30 K/min heating rate, a 70 eV ionization energy, and SIR detection of several ions (4, 13-18, 25-32, 35-46 in one run and 4, 32, 43-46, 50-52, 55-58, 60, 65, 68, 73, 78, 91, 96, 105, 106 in another run). The response of each ion was divided by that of helium (m/z= 4) and afterwards the corresponding minimum value was subtracted from each response.

The TG-IR runs were carried out on a Perkin Elmer STA6000 and a Nicolet 6700 FT-IR using air as carrier gas, a mass sample of around 12 mg and at 30 K/min heating rate. The transmittance was measured between 4000 and 600 cm^{-1}.

3. RESULTS AND DISCUSSION

Most of the TG runs were carried out on the Mettler Toledo Thermobalance in the aluminium crucible. Figures 1 and 2 show the first experimental TG plots for the combustion of pure olive oil, which must be analyzed in order to understand subsequent runs and the proposed kinetic model. Figure 1a shows the TG runs carried out on the Mettler Toledo (M-T) instrument for combustion and pyrolysis of pure olive oil (data for the latter were obtained elsewhere [3]) at 10 K/min and for a 5 mg initial mass. As observed, the thermal decomposition is faster under oxidative conditions. It is possible that a carbonaceous residue has been formed by oxidation, whose subsequent combustion results in the presence of a fraction in the oxidation run curve on the right of the pyrolysis run curve. That this residue has been possibly formed should be confirmed by means of other techniques, such as TG-MS and TG-IR, since other explanations are also possible. Figure 1b shows the results of three runs carried out at 5, 10 and 20 K/min on an initial mass of 5 mg. It can be observed that the curves intersect, which also occurs in other series of runs. The exothermal nature of the combustion run can be confirmed from the variation in the temperature increment of the DTA corresponding to 20 K/min, by noticing that there is an increase in temperature throughout the entire process and a peak that coincides with the weight that has been lost. Figure 1c shows the results of three TG runs carried out under the same operating conditions but varying the initial masses. It can be seen that there is a considerable difference between the experimental curves obtained for 1 and 5 mg on the one hand, and 10 mg on the other. Concerning the experimental data, Figure 1d shows the results of the TG (weight fraction) and DTG (mass fraction increment in volatiles per unit temperature increment, $\Delta V/\Delta T$) for a run carried out at 5 K/min on 5 mg of oil. Three peaks are visible at 600, 700 and 800 K (the label "cal" refers to data calculated by means of the proposed model). The results of two other runs carried out under the same operating conditions are shown in Figures 2a and 2b. Small differences between the DTG curves can be observed, which demonstrates again that the runs are not exactly reproducible. Figure 2c shows calculated results for the decomposition steps involved in the reactions that are proposed in the following sections. Figure 2d shows the results of a run carried out at 20 K/min on 5 mg of oil. In light of the previous results, the following aspects deserve comment: a) at least three decomposition steps can be considered based on the presence of three peaks in the DTG runs, b) the run carried out on 10 mg has a curve that is very separated from the curves of the other two runs carried out on 1 mg and 5 mg, probably as a consequence of the large sample mass, which could cause the temperature of the samples to be different to that programmed (the effect of sample mass must be considered to obtain acceptable results) c) there could be a factor that leads to random behavior and provokes crossing of the curves. This can be attributed to a vaporization process, as in the case of the pyrolysis runs [3]. Previous studies have revealed that the vaporization processes exhibit a random variation in weight loss vs. temperature in dynamic TG runs done within the interval of vaporization, which is the result of irregular diffusion of vapours along the length of the crucible [20,21]. No other reasons for the random behavior have been found.

Figures 1 and 2

Figure 3 shows the results of runs also carried out on the Mettler Toledo Thermobalance, but now on 1 mg of pure olive oil. The DTA in Figure 3a is for the 20 K/min run and is indicative of an exothermic process throughout the entire run. The first of the three peaks in the DTG plot in Figure 3c is very broad, so presumably four decomposition steps, two decomposition steps corresponding to the broad peak and two decomposition steps from the following two peaks should be considered when analyzing the experimental data. Figures 3b and 3d show calculated data that will be explained later.

Figure 3

The analysis of the runs carried out at N_2:O_2 = 9:1 atmosphere, the results of the runs carried out with the Perkin Elmer Thermobalance and some results of the dynamic + isothermal runs are presented in Supplementary Material.

Figures 4a to c show the TG curves of runs carried out on pure olive oil, waste olive oil and waste mixed oil, respectively. The overall decomposition is similar in all cases in spite of the thermal treatment undergone by the waste oils. Another TG run carried out on waste olive oil at 10 K/min instead of 20 K/min is shown in Figure 4d.

Figure 4

Before turning to a description of the proposed kinetic model, the TG-MS and TG-IR data will be presented and analyzed since they are useful in identifying the different decomposition steps.

4. ANALYSIS OF TG-MS DATA

Figure 5 shows the results of the TG-MS run carried out on a 5 mg initial mass of pure olive oil at 30 K/min and at a He:O_2 = 4:1 atmosphere (the high heating rate was required to obtain acceptable signals for the evolved ions). The intensity of a number of ions have been measured: water (18), carbon monoxide (28, including ethylene), carbon dioxide (44) and methane (15). It can be seen that the ion corresponding to water appears in the interval 500-750 K, coinciding with the thermal degradation of the olive oil, except in the last step. By contrast, ions of both carbon oxides appear throughout the entire decomposition process, from 500 to 850 K, indicating that the last decomposition step corresponds to the combustion of a carbonaceous residue with formation of carbon oxides and very little or no formation of water.

Considering the remaining TG-MS data, it seems that formaldehyde (ions 29 and 30), acetaldehyde (ions 29 and 43), ethylene (ions 27 and 26, because ion 28 also corresponds to carbon monoxide), acetylene (ions 26 and 25), other hydrocarbons (ions 25, 26, 27, 39, 40 41 and 42) and other oxygenated compounds (ion 57) are formed inside the interval 500-750 K, including methane, as a consequence of the thermal decomposition. The study has been extensive considering all the ions listed in the experimental section. The emission of benzene, toluene or xylenes – ions 78, 91 or 106 – was not observed.

Figure 5

5. ANALYSIS OF THE TG-IR DATA

Figure 6 shows the results obtained in the dynamic run carried out on a 12 mg initial mass of pure olive oil at 30 K/min in air, on the Perkin Elmer TG and the Nicolet FT-IR apparatus. Figure 6a shows the transmittance at time 15.5 min, when the weight loss rate is high. The following peaks have been identified in accordance with NIST data base and Vlachos et al. [22]: 3400-4000 cm^{-1} and 1300-1600 cm^{-1} due to water vapor, 2300-2400 cm^{-1} and 700 cm^{-1} due to CO_2, 2100-2200 cm^{-1} due to CO, 2850-3000 cm^{-1} due to C-H bonds, 1700-1800 cm^{-1} due to C-O bonds and 1150-1250 cm^{-1} due to C-O ester groups.

Figure 6

Figure 6b shows the variation of transmittance vs. time corresponding to a wavelength of 2930 cm^{-1} (C-H bond). Only one broad peak is observed. Similar trends occur in the case of the other wavelengths, except for those corresponding to CO and CO_2 (see Figure 9c where two broad peaks can be observed). This fact confirms the conclusion drawn based on the TG-MS results. The first broad peak in Figure 9c corresponds to decomposition reactions, whereas the second broad peak, only observed for CO_2 in Figure 6c and CO at its characteristic wavelength, correspond to the combustion of a carbonaceous residue accompanied by little or no formation of water and organic compounds. Similar trends were obtained in the case of the waste olive oil and waste mixed oil.

6. KINETIC MODEL

Several kinetic models were considered for the purpose of reproducing the experimental results. Since at least four decomposition steps must be taken into account, the following scheme of four parallel reactions has been proposed (reactions 1A and 1B corresponding to the first broad peak, reactions 2 and 3 for the following peaks in DTG runs):

$$\text{Oil} + O_2 \xrightarrow{1A} v_{1A\infty}\,\text{volatile fraction} + \text{carbonaceous fraction} \qquad \text{(R1A)}$$

$$\text{Oil} + O_2 \xrightarrow{1B} v_{1B\infty}\,\text{volatile fraction} + \text{carbonaceous fraction} \qquad \text{(R1B)}$$

$$\text{Oil} + O_2 \xrightarrow{2} v_{2\infty}\,\text{volatile fraction} + \text{carbonaceous fraction} \qquad \text{(R2)}$$

$$\text{Carbonaceous fraction} + O_2 \xrightarrow{3} v_{3\infty}\,\text{volatile fraction} \qquad \text{(R3)}$$

where $v_{1A\infty}$, $v_{1B\infty}$, $v_{2\infty}$ and $v_{3\infty}$ are the maximum mass fractions of volatile products of reactions 1A, 1B, 2 and 3, respectively, having been produced long after the reactions had gone to completion. Taking into account that the final residue is negligible, the sum of these maximum mass fractions of volatiles must equal 1. The carbonaceous fraction in question is the one produced by any of the reactions 1A, 1B or 2.

This kinetic model is based on the decomposition steps observed and must be considered as a simplification of the complicated network of reactions that take place. This kinetic model must be considered as a correlation of the experimental data obtained.

For every reaction, the conversion degree is calculated as the ratio of the mass fraction of volatiles obtained at any instant during the reaction (V_i) to the corresponding yield coefficient or the mass fraction of volatiles at time infinity ($v_{i\infty}$), or

$$\alpha_i = V_i / v_{i\infty} \qquad i = 1A, 1B, 2 \text{ and } 3 \qquad (1)$$

The kinetic equation of each reaction i can be expressed as

$$d(V_i / v_{i\infty}) / dt = d\alpha_i / dt = k_i (1 - \alpha_i)^{n_i} = k_i (1 - (V_i / v_{i\infty}))^{n_i} \qquad i = 1A, 1B, 2 \text{ and } 3 \quad (2)$$

For reaction 3, the same kinetic model is assumed to apply on the grounds that the carbonaceous residue is formed at low temperatures prior to combustion.

The kinetic constants are obtained from the Arrhenius equation, or

$$k_i = k_{oi} \exp(-E_i / RT) \qquad i = 1A, 1B, 2 \text{ and } 3 \qquad (3)$$

By integrating the above equations, the conversion degrees can be calculated at every instant from a knowledge of the temperature program. The weight or mass fraction measured in the thermobalance (w) is related to the volatiles obtained (V) by:

$$\begin{aligned} \text{Mass fraction} &= 1 - V = 1 - (V_{1A} + V_{1B} + V_2 + V_3) = \\ &= 1 - \left(v_{1A\infty}\alpha_{1A} + v_{1B\infty}\alpha_{1B} + v_{2\infty}\alpha_2 + v_{3\infty}\alpha_3\right) \end{aligned} \qquad (4)$$

Assuming initial values for all the kinetic constants (k_{oi}, E_i, n_i) and maximum mass fractions, $v_{i\infty}$, we calculated the conversion degrees by integrating the differential equations in Eq. (2) above, using Euler's method and small time intervals, as well as optimization with the Solver function in an Excel spreadsheet. We subsequently checked that integration by Euler's method was accurate by decreasing the time interval, which gave the same results. It has also been confirmed that the kinetic parameters obtained by applying the iso-conversional method [23] to a reaction, coincide with those employed in the simulations using Euler's method, for small time intervals of the same order as those used in this work. The objective function (OF) to minimize was the sum of the square differences between the experimental and calculated mass fractions:

$$\mathrm{OF} = \sum_{m=1}^{M}\sum_{j=1}^{N}(\text{mass fraction}_{m,j}^{exp} - \text{mass fraction}_{m,j}^{cal})^2 \qquad (5)$$

where M is the number of runs and N is the number of points in each run.

The validity of the model has been established by calculating the variation coefficient (VC):

$$\mathrm{VC} = 100\sqrt{(\mathrm{OF}/(N_{total} - P))} \,/\, \overline{\text{mass fraction}_{exp}} \qquad (6)$$

where N_{total} and P are the number of data values and parameters fitted, respectively, and $\overline{\text{mass fraction}_{exp}}$ is the average mass fraction that remains inside the crucible, which is close to 0.5. In accordance with the approach proposed in Martín-Gullón et al. [24], the optimization was performed with respect to a 'comparable kinetic constant', K_i*, instead of optimizing k_{oi} directly. This constant was calculated at a reference temperature (T_{ref}) around the maximum decomposition rate, after the inclusion of a factor $(0.64)^{ni}$, as:

$$K_i^* = k_i(0.64)^{n_i} = (k_{oi}\exp(-E_i/RT_{ref}))(0.64)^{n_i} \qquad (7)$$

The number 0.64 was introduced to weaken the dependence of the reaction order and the other kinetic parameters on each other [24]. From the optimized parameters K_i^*, E_i and n_i, the values of k_{oi} can be deduced. Note that the parameter K_i^* is only used and valid for correlation purposes, since it facilitates optimization and decreases the computational time.

The optimization parameters for reactions 1A, 2 and 3 were K_i^*, E_i, n_i and $v_{i\infty}$. As for reaction 1B, they were E_{1B}, n_{1B}, $v_{1B\infty}$ and the value of K_{1B}^* in each run. The fact that K_{1B}^* varies between runs can be justified if a vaporization process takes place during the devolatilization process; it has been established that the pre-exponential factor depends on the initial mass in the vaporization process, and that it can vary between similar runs due to a random process that depends on the heating rate [20,21].

To deduce the best kinetic parameters that minimize the objective function so that the experimental and calculated TG curves match, the data obtained with the Mettler

Toledo TG apparatus at a N_2:O_2 = 4:1 atmosphere were used as initial values. The same set of parameters was used in the runs carried out on the Perkin Elmer TG.

Table 2 shows the optimized pre-exponential factors k_{o1B} obtained in each run and Table 3 shows the kinetic parameters obtained for each reaction. With the optimized parameters, the mass fraction curves were calculated and plotted together with their experimental values, both TG and DTG, in Figures 1 to 4. The same was done in the case of the other tests. It can be seen that the calculated results agree well with the experimental ones in most cases (reason why the small differences cannot be observed), demonstrating that the proposed model is useful for correlating the data. Figures 2c and 3d show the variation in volatile mass fraction for the four reactions: reactions 1A and 1B take place in the interval of 500-750 K, whereas reaction 2 and 3 take place in 700-800 K and 750-850 K, respectively.

The variation coefficient of each run was calculated using a mean value for the mass fraction of 0.5 in all the runs. Table 2 shows these results, where it can be seen that in the N_2:O_2 = 4:1 runs the variations are smaller than 10 %, except in the case of the two runs carried out on the Perkin Elmer TG at 5 K/min. This makes us confident about the ability of our kinetic model to correlate the experimental results obtained from the two different TG apparatus. It is worth noting, however, that in the two runs where the VC exceeds 10 %, the experimental conversions are greater than those predicted by the model, and therefore the model is useful to check that a conversion is obtained or surpassed.

The following analysis can be done based on the obtained kinetic parameters:

- Reaction 1A is the most important and contributes up to 50.2 % of the initial mass, whereas reaction 1B contributes only 18.7%. These two reactions have similar apparent activation energies – around 125 kJ/mol – and their reaction orders are 1.73 for reaction 1A, and 1.07 for reaction 1B. The obtained parameters are the result of the best correlation of the data, and consequently they have no clear physical meaning. This fact may indicate that the proposed scheme is an over-simplification of the real process. The relatively low apparent activation energy of reaction 1A and its reaction order of 1.73 indicate that there are many consecutive and parallel reactions giving rise to these correlation values.

-Where reaction 1B is concerned, the vaporization effect together with consecutive and parallel reactions give rise to a reaction order close to 1, a value between zero for vaporization processes and orders greater than unity that can be found in literature for chemical reactions. The activation energy also has a low value, but is greater than that of a volatilization process (30-70 kJ/mol). It is curious that in the pyrolysis of olive oil [3] using the same thermobalance, there was also a first vaporization + reaction process, with a reaction order of 0.606 and an apparent activation energy of 112 kJ/mol, whereas in the case of reaction 1B in the combustion process, the reaction order is 1.07 and the apparent activation energy is 124 kJ/mol, a value close to 112 kJ/mol. Perhaps there is a similarity between the processes of pyrolysis and combustion, with the difference being that the oxidation of the reacting mass gives rise to an increase in the overall reaction rate because of oxygenated radicals.

The kinetic parameters of reactions 1A and 1B are comparable with those (reaction order around 1 and activation energy around 85-100 kJ/mol) obtained in the first step of the decomposition proposed by Santos et al. [12] and also comparable to those obtained by Gouveia de Souza et al. [11].

- For reaction 2, the apparent activation energy is high, 389 kJ/mol, and so is the reaction order, 3.31. These results have opposing effects: high activation energies mean sharp peaks in a DTG run, whereas high reaction orders mean broad peaks. Perhaps lower activation energies and reaction orders are also acceptable. Nevertheless, the obtained correlation values are optimal – also upon taking into account the other three decomposition steps and all the dynamic and dynamic + isothermal runs. Gouveia de Souza et al. [11] proposed activation energies of 205-300 kJ/mol and reaction orders of 2.0 or 2.1.

- Reaction 3 corresponds to the combustion of a carbonaceous residue, which is in keeping with the comparison between pyrolysis and combustion runs, and considering the TG-MS and TG-IR results. The activation energy and reaction order are 240 kJ/mol and 1.04, respectively, which are acceptable values for combustion processes. Gouveia de Souza et al. [11] proposed activation energies of 300-380 kJ/mol and reaction orders of around 1.9-2.1, which are similar to those proposed by Santos et al. [12].

Vecchio et al [14] presented DTG data of triglycerides: tristearate, trioleate, trilinoleate and trilinolenate. They observed three steps of decomposition: a first wide one, which can be decomposed in two for trioleate, a second step with an acute peak and a third step, which corresponds to the burnout of the carbonaceous residue.

The data presented in Table 3 correspond to a N_2:O_2 = 4:1 and N_2:O_2 = 9:1 atmosphere. The same set of parameters was used in the correlation of runs carried out at N_2:O_2 = 9:1 and N_2:O_2 = 4:1. However, several aspects are worth commenting:

- The pre-exponential factor k_{o1B} of each run has been optimized, as was done in N_2:O_2 = 4:1 runs.

- It seems that less of the carbonaceous residue forms than in the case of N_2:O_2 = 4:1 runs, so that the mass fractions of the other reactions (1A, 1B and 2) increase, as shown in Table 3.

- For the runs carried out on 5 mg samples, the pre-exponential factor of reactions 1A, 2 and 3 decrease with respect to N_2:O_2 = 4:1 runs by a factor of 0.32, which is obtained experimentally by optimization when the corresponding experimental data are correlated. This factor corresponds to a reaction order of 1.64 with respect to the oxygen partial pressure, and was calculated as follows:

$$\frac{\log 0.32}{\log\left[\frac{P_{O2}\ \text{for}\ N_2:O_2=9:1}{P_{O2}\ \text{for}\ N_2:O_2=4:1}\right]}=\frac{\log 0.32}{\log\left[\frac{0.1}{0.2}\right]}=1.64 \qquad (8)$$

This reaction order is greater than unity probably as a consequence of diffusion of oxygen inside the crucible, which causes the oxygen concentration in the surface of the oil to be less than the external oxygen concentration.

- For the runs carried out on 1 mg samples, the pre-exponential factors of reactions 2 and 3 decrease by the same factor, 0.32. However, for reaction 1A, the pre-exponential factor is the same as in the N_2:O_2 = 4:1 run. This would indicate that in the case of reaction 1A, the oxygen is probably required as an initiator in oxygenated radical formation and as a reactant. For the runs carried out on 1 mg and 5 mg samples at N_2:O_2 = 4:1, and on 1 mg at N_2:O_2 = 9:1, there is sufficient oxygen present to achieve the maximum degradation rate, whereas for 5 mg at N_2:O_2 = 9:1 there is not, and thus the reaction proceeds more slowly. All these considerations highlight the complexity of the process.

Figure 4 shows the experimental and calculated results obtained for pure olive oil, waste olive oil and waste mixed oil by means of the same correlation procedure. This means that approximately the same kinetic model can be applied, although for certain waste mixed oils several runs should be done to confirm or modify the kinetic parameters and the mass fraction of volatiles involved in each reaction.

The values of the pre-exponential factor k_{o1B} have been correlated roughly by means of a parameter P, which is defined as:

$$P = (\text{initial mass in mg})^{a} \cdot (\text{heating rate in K/min})^{b} \cdot (\text{height in cm})^{c} \cdot (\text{diameter in cm})^{d}$$

The optimal values of a, b, c and d that obtain the best correlation between k_{o1B} and P are as follows: a= -2.3, b=-0.68, c=-3.5 and d=16.0. A logarithmic plot of k_{o1B} vs. P is shown in Figure 7. The values of exponents a,b,c,d reveal a trend in the variation of process 1B, when vaporization is included. If the process were only vaporization of a pure substance in a pure molecular diffusion process, the expected values would be the following: a= -1; b=0; c=-1; d=2. The obtained values differ from these, but the positive and negative values follow the expected trend. The convective phenomena produced by temperature gradients, the formation of small drops at the end of the run and the shape of the crucible, which is not exactly cylindrical, can alter molecular diffusion inside the crucible, which is one of the factors controlling the vaporization rate [20,21].

Figure 7

7. APPLICATION OF THE KINETIC MODEL

The system of equations that we have deduced is useful to characterize the decomposition of olive oil, waste olive oil and more approximately the decomposition of waste mixed oil. However, there are some aspects that merit consideration:

1. The mass fraction of the last reaction (combustion of the carbonaceous material) can depend on the combustion conditions and vary between 0.13 for N_2:O_2 = 4:1 and 0.08 for N_2:O_2 = 9:1. For intermediate conditions, an interpolation can be done. The mass

fraction of the other reactions must be recalculated so that the sum of all fractions is equal to unity.

2. The value of the pre-exponential factor k_{o1B} depends on operating conditions, so extrapolation of the TG data to industrial conditions may be risky. A first approximation would imply assuming that reactions 1A and 1B are similar, so that the kinetic parameters of reaction 1A can be used for the sum of the mass fractions of reactions 1A and 1B. An analysis of the operating conditions of the industrial process can also be done to estimate the equivalent diffusion length (mass transfer coefficient/diffusivity). This can be compared with the height of the crucibles that are used, in order to establish whether the vaporization process implied in reaction 1B is faster or slower than reaction 1A. In any case, the proposed approximation may be valid.

8. CONCLUSIONS

Four decomposition steps have been suggested for correlating the complex system of reactions involved in the combustion of olive oil. Reactions 1A and 1B take place at 500-750 K, reaction 2 at 700-800 K and reaction 3 at 750-850 K. In reaction 1B, which corresponds to a vaporization + reaction process, the observed random behavior is deduced to be the result of the vaporization process. The last reaction corresponds to the combustion of a carbonaceous residue.

The obtained kinetic parameters have been instrumental to satisfactorily simulating the experimental results.

The kinetic model might also be roughly applicable to waste olive oil and waste mixed oil, although where waste mixed oil is concerned, more runs should be done to confirm or vary the kinetic parameters.

The kinetic study carried out on different initial masses using two distinct TG apparatus together with TG-MS and TG-IR data, is useful for analyzing the thermal behavior of liquids and for explaining a number of random results in the TG and DTG data.

AUTHOR INFORMATION

Corresponding Author

*Phone: +34 96 590 35 46, Fax: +34 96 590 38 26, e-mail: rafael.font@ua.es.

ACKNOWLEDGMENTS

Support for this work was provided by PROMETEO/2009/043/FEDER of Generalitat Valenciana (Spain) and CTQ2008-05520 (Spanish MCI/research).

REFERENCES

[1] K. D. Maher, D. C. Bressler, Pyrolysis of triglyceride materials for the production of renewable fuels and chemicals, Bioresource Technol. 98 (2007) 2351-68.

[2] K. Jansson, T. Wampler, C. Zawodny, Pyrolysis GC/MS used to profile cracking products of bio-oils. Technical Program- Pittcon (2007) (date: 05/09/2012; http://www.analytix.co.uk/Products/Pyrolysis/CDS_pyrolysis_applications/Biofuels_Pittcon_paper.pdf).

[3] R. Font, M.D. Rey, Kinetics of olive oil pyrolysis, J. Anal. Appl. Pyrolysis. 103 (2013) 181-188.

[4] A. G. D. Santos, V. P. S. Caldeira, M. F. Farias, A. S. Araújo, L.D. Souza, A. K. Barros, Characterization and kinetic study of sunflower oil and biodiesel, J. Therm. Anal. Calorim. 106 (2011) 747-751.

[5] I. M. S. Correia, M. J. B. Souza, A. S. Araújo, E. M. B. D. Sousa, Thermal stability during pyrolysis of sunflower oil produced in the northeast of Brazil, J. Therm. Anal. Calorim. 109 (2012) 967-974.

[6] A. C. R. Melo, A. S. Araujo, E.F.B. Silva, R. M. Oliveira, V. J. Fernandes Jr, G. E. Luz Jr., A. G. Souza, Kinetic behavior of sunflower oil pyrolysis over mesoporous materials, Fuel Process Technol. 92 (2011) 1340-1344.

[7] S. Vecchio, L. Cerretani, A. Bendini, E. Chiavaro, Thermal decomposition study of monovarietal extra virgin olive oil by simultaneous thermogravimetry/differential scanning calorimetry: relation with chemical composition, J. Agric. Food Chem. 57 (11) (2009) 4793-4800.

[8] F. Kotti, E. Chiavaro, L. Cerretani, C. Barnaba, M. Gargouri, A. Bendini, Chemical and thermal characterization of Tunisian extra virgin olive oil from Chetoui and Chemlali cultivars and different geographical origin, Eur. Food Res. Technol. 228 (5) (2009) 735-742.

[9] L. S. Tran, B. Sirjean, P-A Glaude, R. Fournet, F. Battin-Leclerc, Progress in detailed kinetic modeling of the combustion of oxygenated components of biofuels, Energy 43 (2012) 4–18.

[10] J. Dweck, C. M. S. Sampaio, Analysis of the thermal decomposition of commercial vegetable oils in air by simultaneous TG/DTA, J. Therm. Anal. Calorim. 75 (2004) 385-391.

[11] A. Gouveia de Souza, J. C. Oliveira Santos, M. M. Conceição, M. C. Dantas Silva, S. Prasad, A thermoanalytic and kinetic study of sunflower oil, Braz. J. Chem. Eng. 21 (2004) 265-273.

[12] J. C. O. Santos, I. M. G. Santos, M. M. Conceição, S. L. Porto, M. F. S. Trindade, A. G. Souza, S. Prasad, V. J. Fernandes Jr., A. S. Araújo, Thermoanalytical, kinetic and rheological parameters of commercial edible vegetable oils, J. Therm. Anal. Calorim. 75 (2004) 419-428.

[13] X. Zhengwen, Kinetic study on pyrolysis and combustion of cooking oil tar under different air concentrations by using Macro-TG-FTIR analysis, Disaster Advances. 5(4) (2012) 1520-1524.

[14] S. Vecchio, L. Campanella, A. Nuccilli, M. Tomassetti, Kinetic study of thermal breakdown of triglycerides contained in extra-virgin olive oil, J. Therm. Anal. Calorim., 91 (2008) 51-56.

[15] M. Tomassetti, G. Favero, L. Campanella, Kinetic thermal analytical study of saturated mono-, di- and tri-glycerides, J. Therm. Anal. Calorim., 112 (2013) 519-527.

[16] A. K. Burnham, R. L. Braun, Global kinetic analysis of complex materials, Energy Fuels 13(1) (1999) 1-22.

[17] E. Ranzi, A. Cuoci, T. Faravelli, A. Frassoldati, G. Migliavacca, S. Pierucci, S. Sommariva, Chemical kinetics of biomass pyrolysis, Energy Fuels 22 (2008) 4292-4300.

[18] J. E. White, W. J.Catallo, B. L. Legendre, Biomass pyrolysis kinetics: a comparative critical review with relevant agricultural residue case studies, J. Anal. Appl. Pyrolysis. 9 (2011) 1-33.

[19] M. Grønli, M.J. Antal, G. Varhegyi, A round-robin study of cellulose pyrolysis kinetics by thermogravimetry, Ind. Eng. Chem. Res. 38 (1999) 2238-2244.

[20] R. Font, M.F. Gómez-Rico, N. Ortuño, Analysis of the vaporization process in TG apparatus and its incidence in pyrolysis, J. Anal. Appl. Pyrolysis. 91 (2011) 89-96.

[21] R. Font, J. Moltó, N. Ortuño, Kinetics of tetrabromobisphenol A pyrolysis. Comparison between correlation and mechanistic models, J. Anal. Appl. Pyrolysis. 94 (2012) 53-62.

[22] N. Vlachos, Y. Skopelitis, M. Psaroudaki, V. Konstantinidou, A. Chatzilazarou, E. Tegou, Applications of Fourier transformed-infrared spectroscopy to edible oils, Anal. Chim. Acta 573–574 (2006) 459–465.

[23] S. Vyazovkin, A. K. Burnham, J. M. Criado, L. A. Pérez-Maqueda, C. Popescu, N. Sbirrazzuoli, ICTAC Kinetics Committee recommendations for performing kinetic computations on thermal analysis data, Thermochim. Acta 520 (2011) 1-19.

[24] I. Martín-Gullón, M.F. Gómez-Rico, A. Fullana, R. Font, Interrelation between the kinetic constant and the reaction order in pyrolysis, J. Anal. Appl. Pyrolysis 68-69 (2003) 645-655.

LIST OF TABLES

Table 1. Elemental analysis of the samples.

Table 2. Operating conditions and values of k_{o1B}

Table 3. Kinetic parameters for a N_2:O_2 = 4:1 and a N_2:O_2 = 9:1 atmosphere.

FIGURE LEGENDS

Figure 1. Variation of weight fraction vs. temperature for runs carried out on different initial masses of pure olive oil at different heating rates.

Figure 2. Variation of weight fraction vs. temperature for runs carried out on 5 mg of pure olive oil at different heating rates (in Figure 2c: 1A, 1B, 2 and 3 is the weight fraction of volatiles evolved in reactions 1A, 1B, 2 and 3).

Figure 3. Variation of weight fraction vs. temperature for runs carried out on 1 mg of pure olive oil at different heating rates (in Figure 3d: 1A, 1B, 2 and 3 is the weight fraction of volatiles evolved in reactions 1A, 1B, 2 and 3).

Figure 4. Variation of weight fraction vs. temperature for pure olive oil and waste oils.

Figure 5. Variation of mass fraction and evolution of gases detected in the TG-MS run carried out on pure olive oil.

Figure 6. IR spectrum of the gases and volatiles evolved in a TG-IR run.

Figure 7. Variation of k_{o1B} vs. parameter P.

A kinetic model, including vaporization and reaction, is proposed

Two TG apparatus have been used, so the results can be compared

The kinetic model is supported by TG-MS and TG-IR runs.

	Carbon (%)	Hydrogen (%)	Oxygen (%)	Nitrogen (%)	Sulfur (%)	Net calorific value (kcal/kg)
Olive oil	77.5	11.6	10.9	0.0	0.0	8884
Waste olive oil	77.2	11.6	11.2	0.0	0.0	8859
Waste Mixed oil	76.9	11.6	11.5	0.0	0.0	8784

Table 2

	N_2:O_2 ratio	M (mg)	Run	Heating rate (K/min)	TG Apparatus	Crucible Material	Height (cm)	Int. Diam. (cm)	k_{01B} (s^{-1})	Parameter P	VC (%)
Olive oil	4 : 1	4.791	D	20	Mettler Toledo	Aluminium	0.41	0.55	$7.324 \cdot 10^{8}$	$2.18 \cdot 10^{-7}$	4.1
Waste olive oil	4 : 1	6.187	D	20	Mettler Toledo	Alumina	0.425	0.47	$3.481 \cdot 10^{7}$	$1.56 \cdot 10^{-7}$	7.1
Waste mixed oil	4 : 1	5.643	D	20	Mettler Toledo	Alumina	0.425	0.47	$1.361 \cdot 10^{7}$	$1.96 \cdot 10^{-7}$	7.9
Olive oil	4 : 1	5.024	D	10	Mettler Toledo	Aluminium	0.41	0.55	$1.354 \cdot 10^{7}$	$2.19 \cdot 10^{-7}$	4.1
Waste olive oil	4 : 1	5.020	D	10	Mettler Toledo	Aluminium	0.41	0.55	$2.513 \cdot 10^{7}$	$2.19 \cdot 10^{-7}$	4.7
Olive oil	4 : 1	4.996	D	10	Mettler Toledo	Aluminium	0.41	0.55	$2.468 \cdot 10^{7}$	$2.22 \cdot 10^{-7}$	4.7
Olive oil	4 : 1	5.242	D	5	Mettler Toledo	Aluminium	0.41	0.55	$7.257 \cdot 10^{7}$	$2.22 \cdot 10^{-7}$	5.1
Olive oil	4 : 1	1.120	D	20	Mettler Toledo	Aluminium	0.41	0.55	$4.682 \cdot 10^{9}$	$7.96 \cdot 10^{-6}$	4.7
Olive oil	4 : 1	1.095	D	10	Mettler Toledo	Aluminium	0.41	0.55	$5.945 \cdot 10^{9}$	$9.49 \cdot 10^{-6}$	7.2
Olive oil	4 : 1	1.047	D	5	Mettler Toledo	Aluminium	0.41	0.55	$7.508 \cdot 10^{9}$	$1.20 \cdot 10^{-5}$	6.9
Olive oil	4 : 1	5.025	D + I	10	Mettler Toledo	Aluminium	0.41	0.55	$2.709 \cdot 10^{7}$	$2.18 \cdot 10^{-7}$	4.8
Olive oil	air	5.205	D	20	Perkin Elmer	Alumina	0.645	0.42	$1.104 \cdot 10^{10}$	$4.29 \cdot 10^{-5}$	9.3
Olive oil	air	5.051	D	10	Perkin Elmer	Alumina	0.645	0.42	$5.418 \cdot 10^{9}$	$5.21 \cdot 10^{-5}$	6.8
Olive oil	air	5.138	D	5	Perkin Elmer	Alumina	0.645	0.42	$1.889 \cdot 10^{10}$	$5.63 \cdot 10^{-5}$	19.3
Olive oil	air	10.096	D	20	Perkin Elmer	Alumina	0.645	0.42	$8.099 \cdot 10^{8}$	$8.32 \cdot 10^{-6}$	4.4
Olive oil	air	10.808	D	10	Perkin Elmer	Alumina	0.645	0.42	$1.788 \cdot 10^{8}$	$7.92 \cdot 10^{-6}$	7.5
Olive oil	air	10.855	D	5	Perkin Elmer	Alumina	0.645	0.42	$7.504 \cdot 10^{9}$	$8.83 \cdot 10^{-6}$	7.7
Olive oil	air	10.115	D + I	20	Perkin Elmer	Alumina	0.645	0.42	$7.804 \cdot 10^{8}$	$8.28 \cdot 10^{-6}$	2.9
Olive oil	air	10.966	D + I	10	Perkin Elmer	Alumina	0.645	0.42	$7.466 \cdot 10^{9}$	$7.64 \cdot 10^{-6}$	8.8
Olive oil	air	5.152	D + I	5	Perkin Elmer	Alumina	0.645	0.42	$4.058 \cdot 10^{10}$	$5.59 \cdot 10^{-5}$	21.5
Olive oil	9 : 1	5.081	D	20	Mettler Toledo	Aluminium	0.41	0.55	$5.728 \cdot 10^{7}$	$1.89 \cdot 10^{-7}$	8.5
Olive oil	9 : 1	5.006	D	10	Mettler Toledo	Aluminium	0.41	0.55	$4.634 \cdot 10^{7}$	$2.20 \cdot 10^{-7}$	4.2
Olive oil	9 : 1	4.954	D	5	Mettler Toledo	Aluminium	0.41	0.55	$4.237 \cdot 10^{7}$	$2.55 \cdot 10^{-7}$	3.9
Olive oil	9 : 1	1.113	D	20	Mettler Toledo	Aluminium	0.41	0.55	$1.300 \cdot 10^{8}$	$8.09 \cdot 10^{-6}$	9.3
Olive oil	9 : 1	1.062	D	10	Mettler Toledo	Aluminium	0.41	0.55	$1.273 \cdot 10^{8}$	$1.02 \cdot 10^{-5}$	4.9
Olive oil	9 : 1	1.156	D	5	Mettler Toledo	Aluminium	0.41	0.55	$2.781 \cdot 10^{9}$	$9.35 \cdot 10^{-6}$	14.0

Table 3

Reaction	Temperature Interval (K)	k_{i0} (s^{-1}) for N_2:O_2 = 4:1 and air	k_{i0} (s^{-1}) for N_2:O_2 = 9:1	E_i (kJ/mol)	n_i	$v_{i\infty}$ for N_2:O_2 = 4:1	$v_{i\infty}$ for N_2:O_2 = 9:1
1A	520-700	$5.979 \cdot 10^{8}$	$0.32 \cdot 5.979 \cdot 10^{8}$ (for 5 mg initial mass) $5.979 \cdot 10^{8}$ (for 1 mg initial mass)	127.3	1.73	0.502	0.532
1B	500-750 (depending on operating conditions)	see Table 2	see Table 2	124.2	1.07	0.187	0.198
2	700-800	$3.788 \cdot 10^{27}$	$0.32 \cdot 3.788 \cdot 10^{27}$	389.3	3.31	0.178	0.188
3	750-850	$5.040 \cdot 10^{13}$	$0.32 \cdot 5.040 \cdot 10^{13}$	240.7	1.08	0.132	0.080

Figure 1

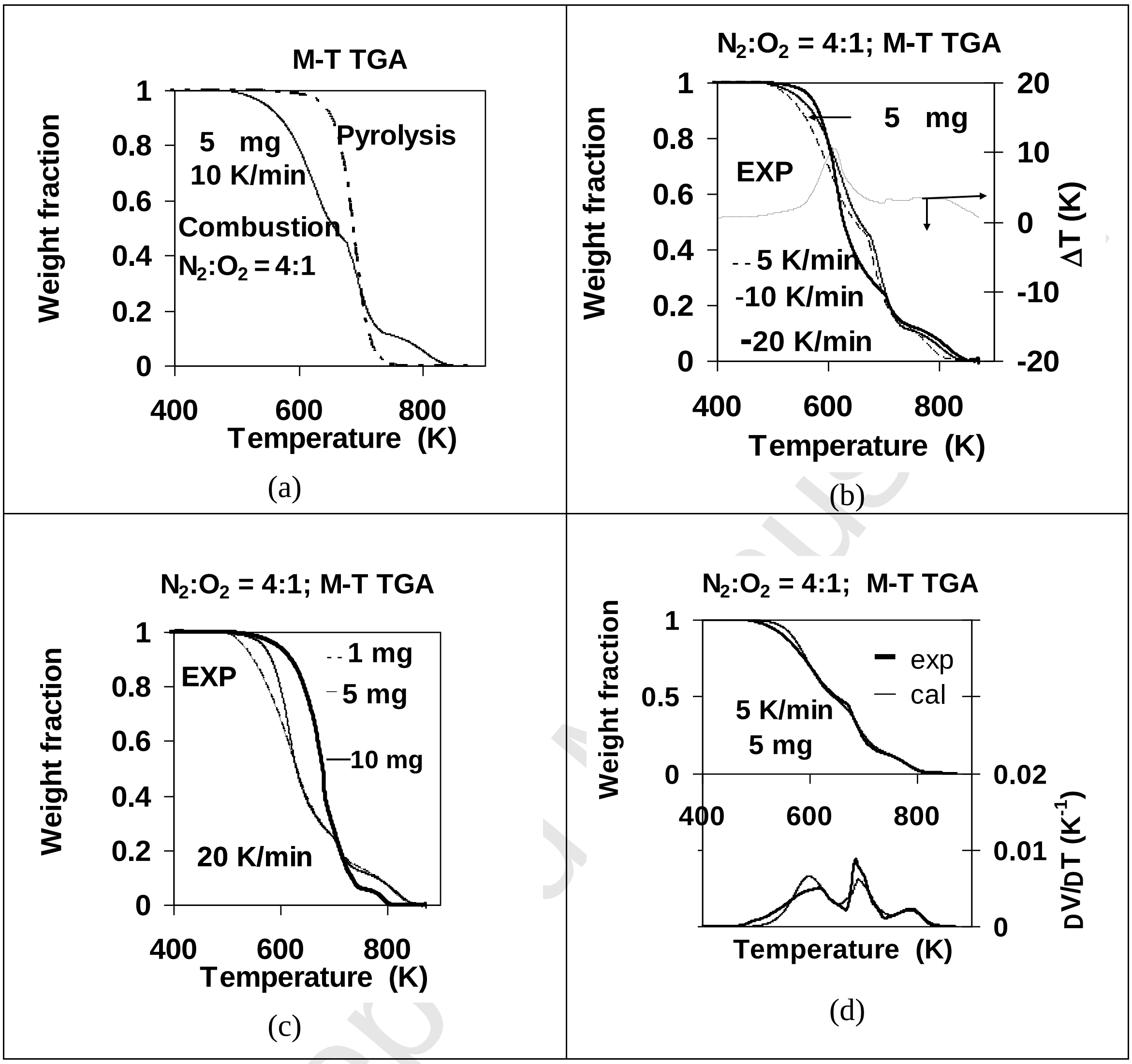
M-T TGA
Weight fraction
1
0.8
0.6
0.4
0.2
0
5 mg
10 K/min
Pyrolysis
Combustion
N_2:O_2 = 4:1
400
600
800
Temperature (K)
(a)
N_2:O_2 = 4:1; M-T TGA
Weight fraction
5 mg
EXP
- - 5 K/min
-10 K/min
-20 K/min
20
10
0
-10
-20
ΔT (K)
400
600
800
Temperature (K)
(b)
N_2:O_2 = 4:1; M-T TGA
Weight fraction
EXP
- - 1 mg
- 5 mg
—10 mg
20 K/min
400
600
800
Temperature (K)
(c)
N_2:O_2 = 4:1; M-T TGA
Weight fraction
1
0.5
0
exp
cal
5 K/min
5 mg
400
600
800
0.02
0.01
0
DV/DT (K^{-1})
Temperature (K)
(d)

Figure 2

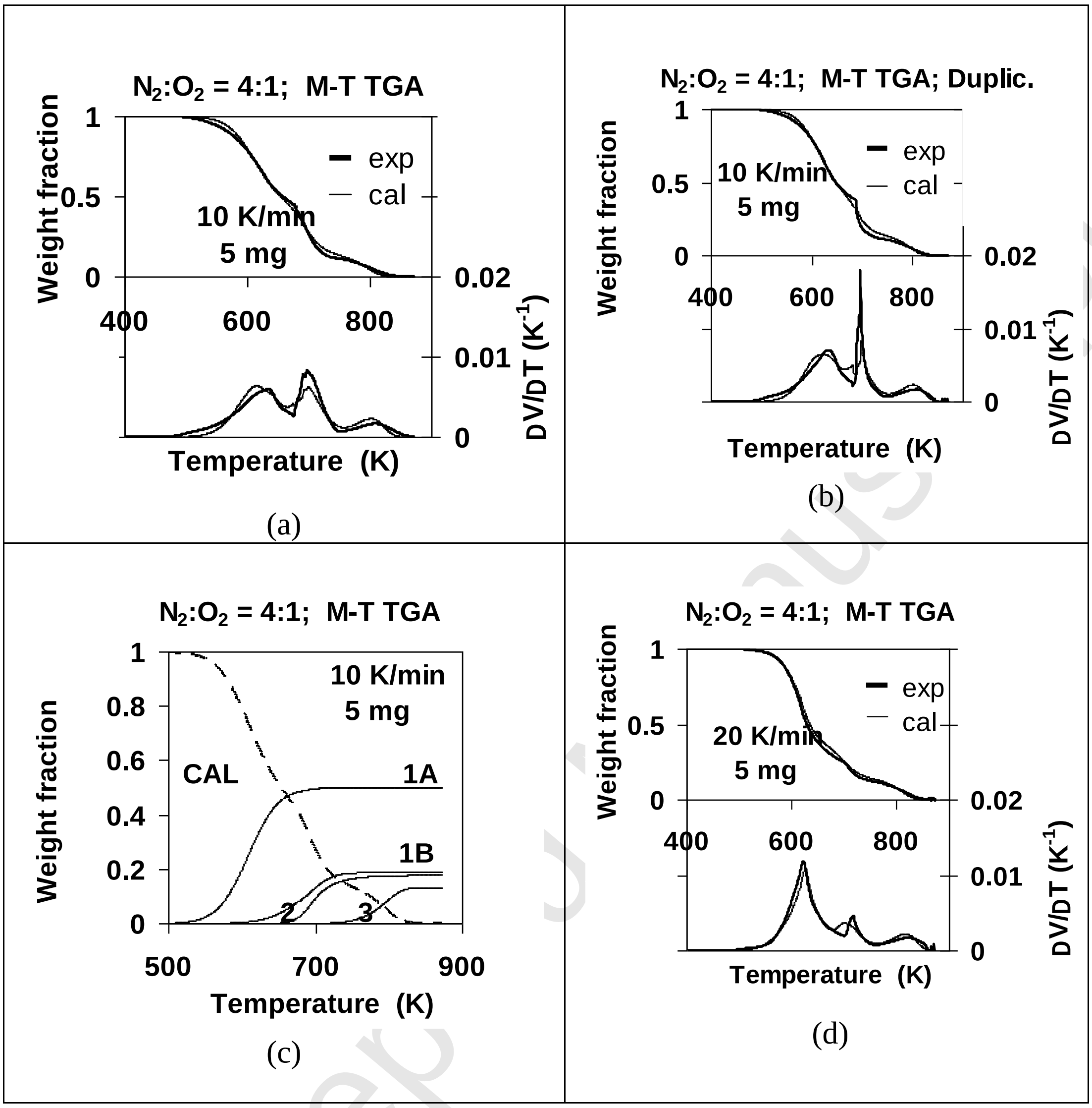

(a)

(b)

(c)

(d)

Figure 3

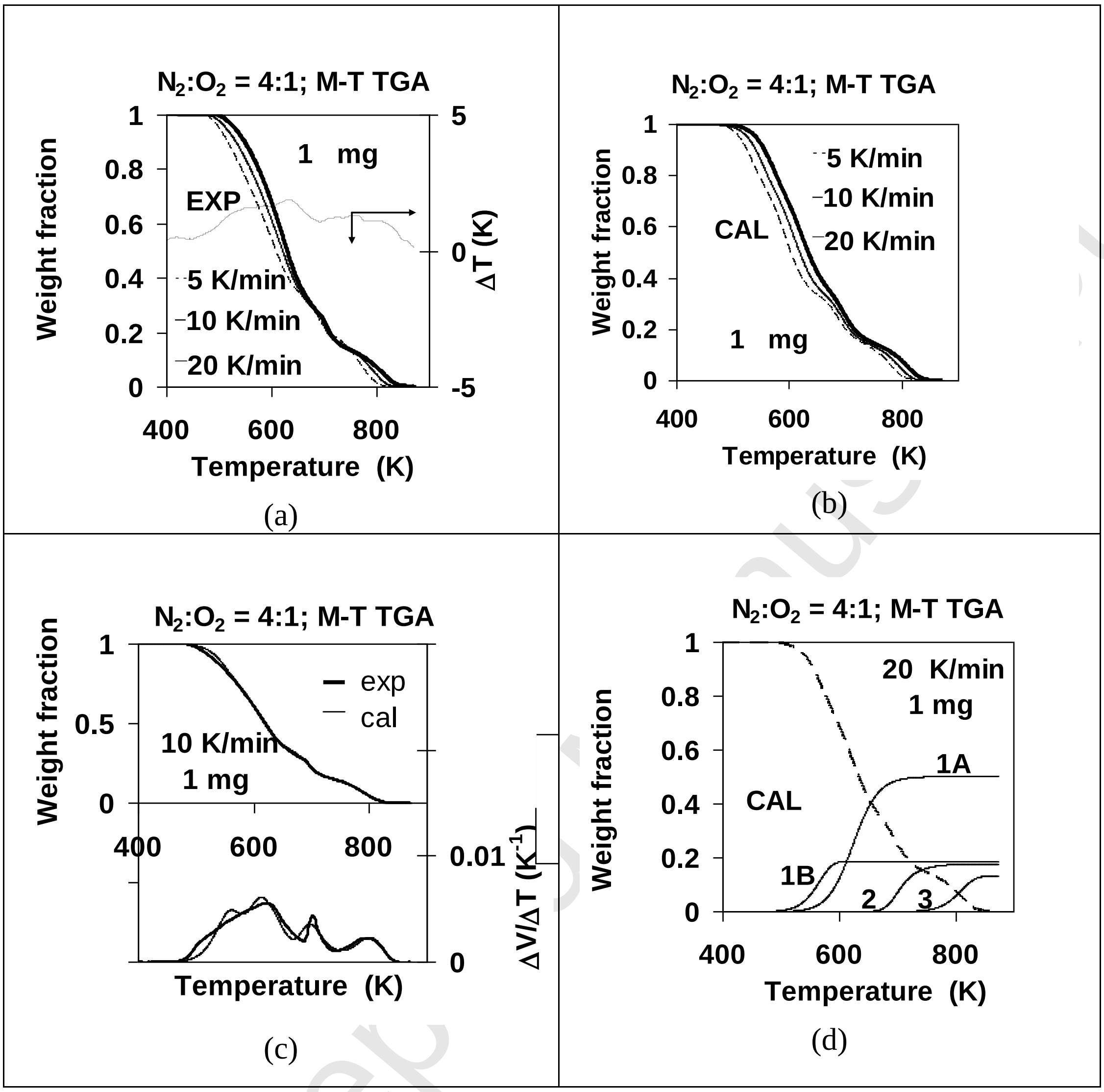

(a)

(b)

(c)

(d)

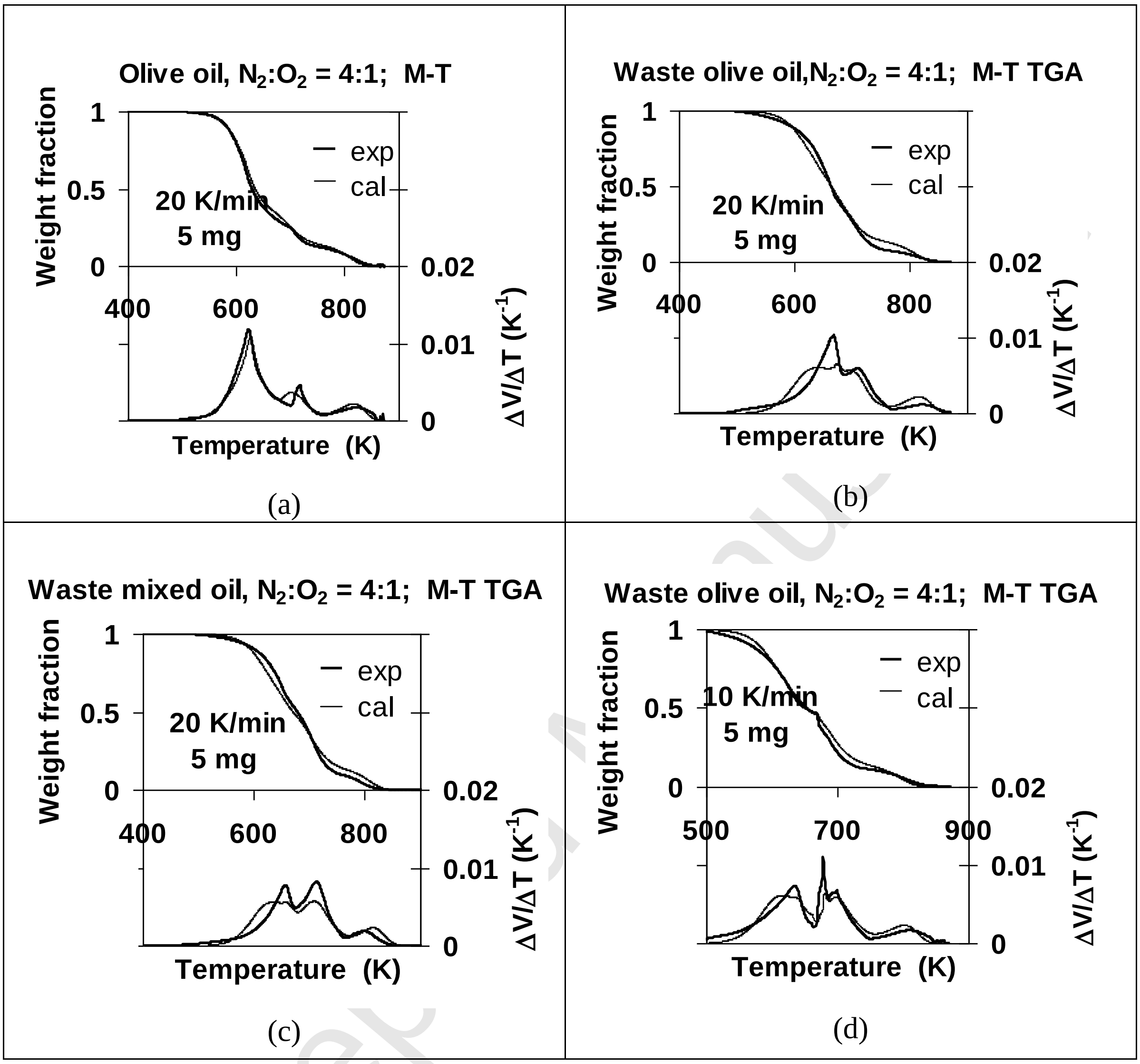
Olive oil, N_2:O_2 = 4:1; M-T
Weight fraction
1
0.5
0
400
600
800
exp
cal
20 K/min
5 mg
0.02
0.01
0
ΔV/ΔT (K^{-1})
Temperature (K)
Waste olive oil,N_2:O_2 = 4:1; M-T TGA
Waste mixed oil, N_2:O_2 = 4:1; M-T TGA
Waste olive oil, N_2:O_2 = 4:1; M-T TGA
10 K/min
500
700
900

(a) (b) (c) (d)

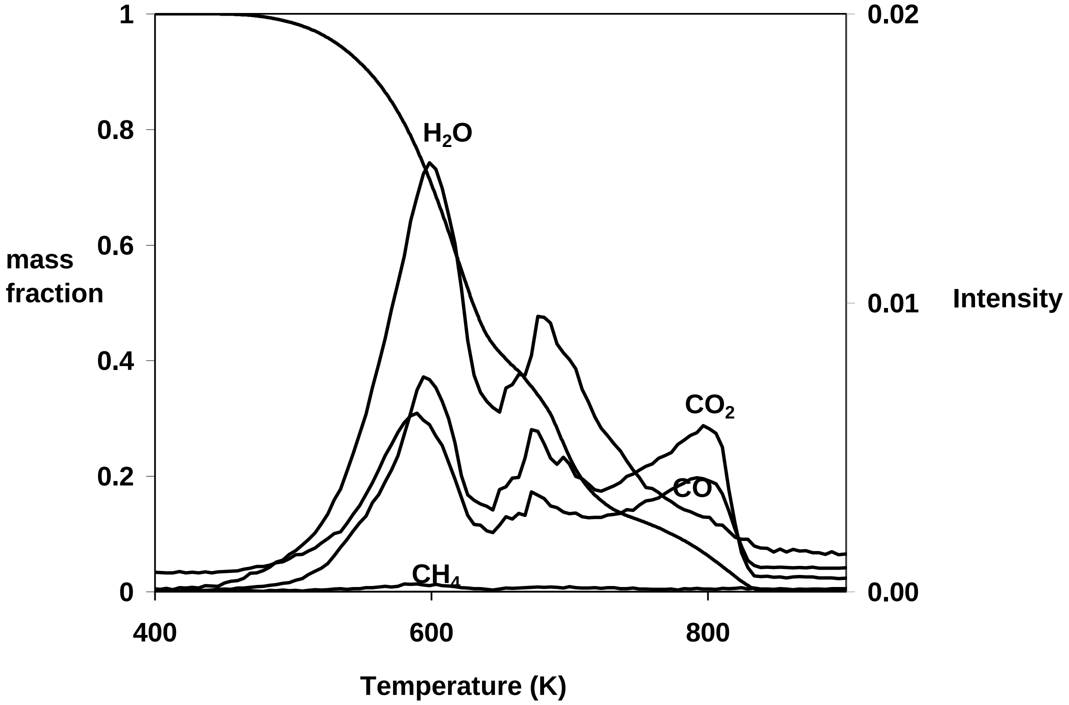
mass fraction
1
0.8
0.6
0.4
0.2
0
0.02
0.01
0.00
Intensity
400
600
800
Temperature (K)
H_2O
CO_2
CO
CH_4

Figure 6

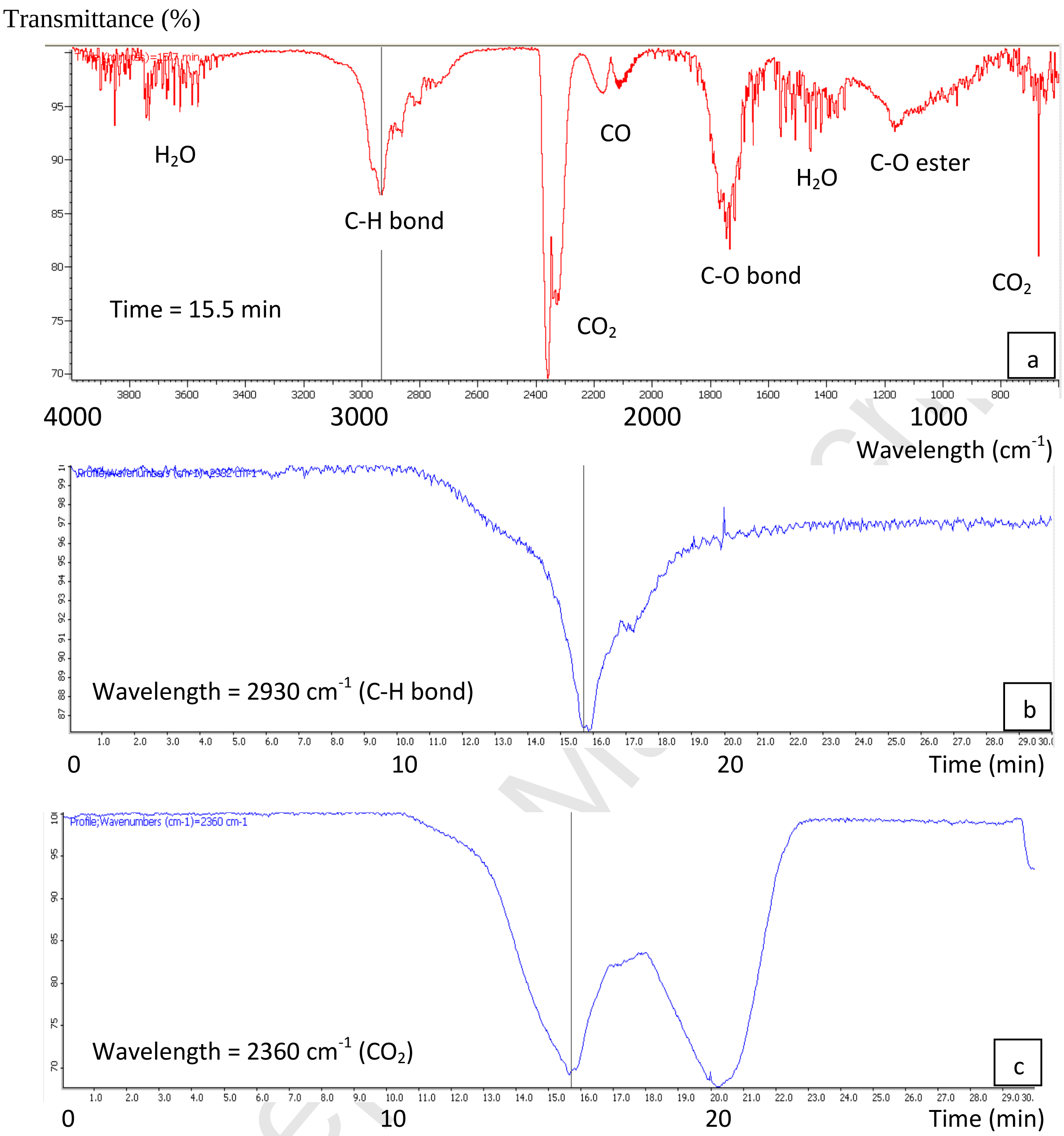
Transmittance (%)
95
90
85
80
75
70
H$_2$O
C-H bond
CO
CO$_2$
C-O bond
H$_2$O
C-O ester
CO$_2$
Time = 15.5 min
a
3800
3600
3400
3200
3000
2800
2600
2400
2200
2000
1800
1600
1400
1200
1000
800
4000
3000
2000
1000
Wavelength (cm^{-1})
Profile,Wavenumbers (cm-1)=2932 cm-1
Wavelength = 2930 cm^{-1} (C-H bond)
b
0
10
20
Time (min)
Profile,Wavenumbers (cm-1)=2360 cm-1
Wavelength = 2360 cm^{-1} (CO$_2$)
c
0
10
20
Time (min)